Feature-point based matching: a sequential approach based on relaxation labeling and relative orientation

Mauricio Galo
UNESP - Universidade Estadual Paulista
FCT, Dep. of Cartography, CP 468
19060-900, Presidente Prudente, SP, Brazil
galo@prudente.unesp.br

Clésio L. Tozzi
UNICAMP - Universidade Estadual de Campinas
FEEC, DCA, CP 6101
13083-970, Campinas, SP, Brazil
clesio@dca.fee.unicamp.br

ABSTRACT

This paper presents a solution for the problem of correspondence and relative orientation (RO) estimation for a pair of images. The solution is obtained by relaxation labeling using multiple metrics applied to image primitives. Besides the use of metrics based on radiometric elements (intensities, gradient, and coefficient of correlation), and on geometry (distance ratios), two additional metrics are considered. One is based on angular relations between primitives and another based on the volume of Matching Parallelepiped (MP) that allows the inclusion of the epipolar geometry constraint directly in the similarity and compatibility computation. The proposed solution was applied to synthetic and real images. The results showed that the use of multiple metrics contribute to the automation of the correspondence process and RO determination, even considering pairs of images subject to convergence, rotation, differences in scale, and presence of repetitive patterns.

Keywords
Point matching, relaxation labeling, epipolar geometry, relative orientation.

1. INTRODUCTION

The search for a robust and automatic solution for the image correspondence problem, or image matching, is one of the most challenging problems in Computer Vision and Digital Photogrammetry. Due to the diversity of applications, sensor types, primitives of interest, and the geometry of the acquisition process, the degree of difficulty of the solution may change.

The solution of the matching problem is facilitated when the geometry of the acquisition system, function of relative camera position and orientation, is known. In that case, it is possible to determine geometric restrictions, which are defined by the epipolar geometry. It is also possible to use rectified images, which reduce the complexity of the matching algorithms from 2D to 1D search.

The geometry of a stereoscopic acquisition system can be expressed by the fundamental matrix, obtained

by the relative orientation (RO) estimation. In some applications, such as the Photogrammetric ones, the acquisition of images is usually made in a well-controlled way, and approximated RO parameters are normally available, as described in Heipke [Hei97] and Tang et al. [Tan96]. However, this condition is not observed in most close-range applications, where the main objective is the 3D reconstruction from images. It is important to mention that in this work it is not considered applications that use 3D range data, as in [Häh02], where the ICP - Iterative Closest Point algorithm is object of analysis.

The determination of RO parameters for an image pair is possible if a set of homologous points is known, and the determination of the homologous pair is facilitated if the RO parameters are available. Despite the fact that automatic correspondence tools are available for some commercial systems [Plu01], there is no guarantee that the automatic RO solution provided is correct, as reported by Habib and Kelley [Hab01].

The integration of the RO and correspondence solution is discussed in Shao [Sha99] and Zhang et al. [Zha94], for example. In [Sha99], although multi-image network (MIN) is considered, approximated values of RO are required. In [Zha94], although epipolar geometry constraints were considered in the RO estimation and correspondence solution, the authors concluded that those restrictions are not

enough to prevent or to diminish the occurrences of false correspondence.

Aiming at a simultaneous solution for the RO and point correspondence for pairs of close-range images, this work presents an approach based on relaxation labeling that combine multiple metrics in the similarity and compatibility computation. Two new metrics were considered to compute similarity and compatibility, one of them based on the volume of Matching Parallelepiped and other on angular relations between primitives. The first metric expresses the interdependency between the correspondence process and RO parameters determination, via epipolar geometry, in an implicit form. The second metric increases the similarities for a candidate pair, if the angular relations in the neighborhood are similar.

Preliminary results considering synthetic images are reported in [Gal99]. In the present paper, additional aspects and experiments considering real images with repetitive patterns and scale differences were also performed and discussed. The algorithm efficiency was evaluated quantitatively by the tax of homologous pairs correctly determined and by the error in the RO parameters.

2. MATCHING PARALLELEPIPED AND EPIPOLAR GEOMETRY

Given the geometry defined by a pair of cameras (see Figure 1) and assuming that the Fundamental matrix F is available, the relation of the homologous points with coordinates $\mathbf{x}_{\{L,R\}}=[x_{\{L,R\}} \; y_{\{L,R\}} \; 1]^t$, measured in the camera coordinate system, may be expressed by the following equation [Bar94, Fau93]:

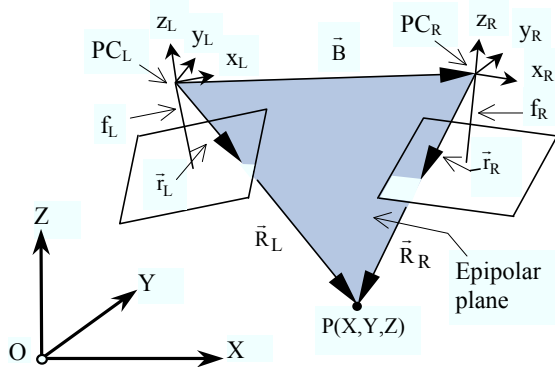$$\mathbf{x}_L^t F \mathbf{x}_R = 0 \quad . \tag{1}$$

Figure 1: Elements of epipolar geometry.

The Fundamental matrix F may be calculated from the Essential matrix E by $F = I_L^t E I_R$, where $I_{\{L,R\}}$ are 3x3 matrices that contain the intrinsic parameters of the cameras, as focal length f and the principal point coordinates (x_0,y_0) [Bar94, Gal97]. The Essential matrix may be obtained by $E = M_L K_B M_R^t$, where

$M_{\{L,R\}}$ are rotation matrices calculated as function of the Euler angles $(\kappa, \; \phi, \; \omega)_{\{L,R\}}$, or from another representation, as quaternion, and K_B is a skew-symmetric matrix, obtained in function of the base components $\vec{B}=[b_x \; b_y \; b_z]^t$ by

$$K_B = \begin{bmatrix} 0 & b_z & -b_y \\ -b_z & 0 & b_x \\ b_y & -b_x & 0 \end{bmatrix} \quad . \tag{2}$$

Being (i,j) a pair of points candidates to the correspondence (Figure 2), the following vectors are determined when considering the epipolar geometry: $\vec{r}_L$ (with extremities in PC_L and i), $\vec{r}_R$ (with extremities in PC_R and j) and the baseline vector $\vec{B}$. From these three vectors translated in order to have a common origin, it is possible to define the parallelepiped shown in Figure 2b, whose volume is determined by the mixed product of these vectors.
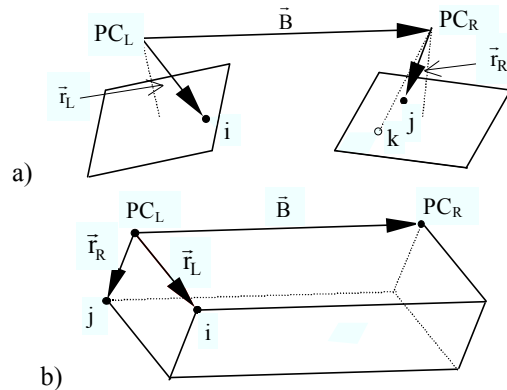

a)

b)

Figure 2: Vectors $\vec{B}$, $\vec{r}_L$ and $\vec{r}_R$ (a) and Matching Parallelepiped (MP) for one pair (i,j) (b).

Given a pair of points (i,j), the Equation 1 will be satisfied just if these points are homologous or if they are located in conjugated epipolar lines. In any of these situations, the edges of the parallelepiped created by these vectors become coplanar, and the vectors become linearly dependents.

So, for a given point (i) on the left image, and another on the right image (j), the volume of the parallelepiped created by the vectors described may be associated to the degree of proximity of the point j to the epipolar line that passes through i, and vice-versa. By this reason the parallelepiped constructed above is called Matching Parallelepiped (MP). The volume of MP (V_{MP}), determined for one generic pair (i,j), and for one given estimate of the Fundamental matrix ($\hat{F}$), may be written by:

$$V_{MP}(\hat{F},i,j) = \left| \mathbf{x}_L^t \hat{F} \mathbf{x}_R \right| . \tag{3}$$

Thus, the value of V_{MP} for the pair (i,j) is directly proportional to the distance from j to the epipolar line defined by i, and vice-versa (from i to the epipolar line defined by j). As a result, this volume may be

used as a metric associated to the attendance of epipolar geometry, and can be incorporated in the relaxation labeling algorithm, since one estimation of $\hat{F}$, which depends on the RO, is available.

3. EPIPOLAR CONSTRAINTS IN THE MATCHING ALGORITHM

The application of relaxation labeling, as it may be seen in Schalkoff [Sch89], Faugeras [Fau93] and Hummel et al. [Hum83], requires the determination of measures of similarity and compatibility between objects.

In the sequence of this session the metrics used for similarity and compatibility computation are discussed and formalized, with emphasis on metrics that express the interdependence of correspondence and RO.

3.1. Incorporation of MP in the similarity computation

The measure of similarity p_{ij} for the pair of candidates (i,j) expresses the degree of the correspondence between i and j. This similarity is usually computed based on one distance, defined by one metric. According to Faugeras [Fau93], the distance d_{ij} between i and j may be related to the similarity p_{ij} by means of different functions. Independently of the function used, the similarity should be high for small values of d_{ij}, and vice-versa. One way to express p_{ij} as function of d_{ij} is through the function

$$p_{ij} = f_s(\alpha, d_{ij}) = k_i /(1 + \alpha d_{ij}) , \qquad (4)$$

where k_i is one normalization constant and α is a positive constant whose value is related to the degree of variation of p_{ij} with d_{ij}.

The metrics used for the determination of the distance d_{ij} depends on the types of primitives extracted from the images. The cross-correlation coefficient, gradient and average intensity differences are usually considered as metrics.

Representing the cross-correlation coefficient by ρ_{ij}, the magnitude of the gradient around i(j) by $grad_{i(j)}$, the average intensity around i(j) by $I_{i(j)}$, and the average intensities of the images by $\bar{I}_i$ and $\bar{I}_j$, the initial similarities for one pair (i,j) may be calculated by $p_{ij}^{(0)} = p_{ij}^{cc} p_{ij}^{grad} p_{ij}^{int}$, where p_{ij}^{grad} and p_{ij}^{int} are calculated using a function in the form of Equation 4 and $p_{ij}^{cc} = \rho_{ij}$. So, the initial similarity $p_{ij}^{(0)}$ may be obtained by:

$$p_{ij}^{(0)} = \rho_{ij}.f_s(\alpha_{grad}, |grad_j - grad_i|).f_s(\alpha_{int}, |I_j - I_i - (\bar{I}_j - \bar{I}_i)|).(5)$$

As the similarity for each pair (i,j) is expressed for the product of three metrics, the result of the Equation 5 will be raised if all the measures of distance also result in high similarities.

Considering that the RO parameters are available, and consequently the $\hat{F}$ matrix, the constraints related to epipolar geometry may be incorporated into the similarity computation, as an additional metric. In consequence, the expression to determine the initial similarities can be rewritten as

$$p_{ij}^{(0)} = p_{ij}^{cc} p_{ij}^{grad} p_{ij}^{int} p_{ij}^{epi} \qquad (6)$$

where

$$p_{ij}^{epi} = f_s(\alpha_{epi}, V_{MP}(\hat{F}, i, j)) , \qquad (7)$$

and V_{MP} is obtained by Equation 3. Note that the component p_{ij}^{epi} can be considered only if $\hat{F}$ is available.

3.2. Incorporation of MP and angular relations in the compatibility computation

The measure of compatibility c_{ij} for the pair (i,j) expresses the level of correspondence between i and j, as well for their neighbors.

Distance relation between neighbors is a possible form to express the compatibility, as described in [Zha94]. Among the possibilities, the equation $c_{ij}^{dist} = \sum_{k=1}^{NN} \delta(i, j; i_k, j_k) /(1 + dist(i, j; i_k, j_k))$ may be considered, where the term $\delta(.)$ is obtained by a Gaussian function written by $\delta(i, j; i_k, j_k) = e^{-r/\varepsilon_r}$, with $r = |d(i, i_k) - d(j, j_k)| / dist(i, j; i_k, j_k)$. In the last equation d (.) represents the Euclidean distance, and dist(.) the average distances between $d(i, i_k)$ and $d(j, j_k)$, i.e., $dist(i, j; i_k, j_k) = [d(i, i_k) + d(j, j_k)] / 2$. It may be observed that the value of r is reached from the pairs (i,j) and (i_k, j_k), where i_k and j_k are, respectively, neighbors of i and j. The value of ε_r in the Gaussian function (δ) is considered as constant, being used in the original reference [Zha94] as a threshold in the difference of relative distance.

In the following sections, two new metrics are detailed, one that considers the angular relations between the neighbors of candidate points and another that expresses the dependence between the correspondence process and RO.

3.2.1. Metrics based on angular ratios

In a similar way that distance relations were used in compatibility computation, one measure of compatibility based on angular relations may be defined. Although angular relations are variant to viewpoint changes, some angular relations are preserved. In the following, this metric is described.

Given a pair of images, I_M and I_N, in which m and n point primitives were independently extracted, two sets of points may be created: **M** and **N**, respectively. From each of these m (in **M**) and n (in **N**) points, NN neighbors may be found, considering the NN nearest points. For each point in **M** and **N**, the ordering of the NN nearest neighbors may be gotten using as criteria, the angle between the horizontal line and each segment that connects i(j) to the NN points. Since these NN directions are ordered, for each point, the angles between the consecutive neighbors may be calculated and stored in the vectors a_i[k] and a_j[k], with k□{1, ...,NN}.

From these two vectors, a measure of compatibility considering angular relations can be defined by:

$$d_{ij}^{ang}[\Delta] = \left| NN - \sum_{k=1,NN} \left(a\_j[k+\Delta]/a\_i[k]\right) \right|, \quad (8)$$

where Δ, with Δ□{0,...,NN-1} expresses the cyclical mutation of the vector a_j, around point j. Then, the distance between i and j is defined by the minimum value of distance $d_{ij}^{ang}[\Delta]$.

Figure 3 illustrates the angular structures for a pair of points, and shows the possible combinations for NN=3. It's important to observe that if (k+Δ)>NN □ (k+Δ)←(k+Δ-NN) in Equation 8.

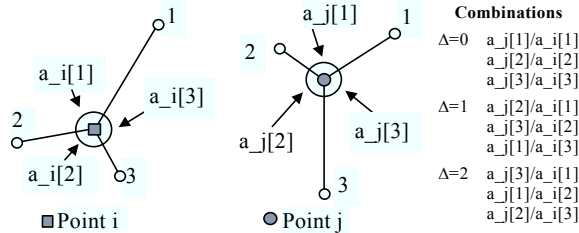Figure 3: Angles between NN(=3) neighbors around each point of the candidate pair (i,j).

It may be observed that in a hypothetical case where the corresponding angles are equal, Equation 8 results in d_{ij}^{ang}=0. Depending on the available angles in a_i[k] and a_j[k], false minimums may occur. In order to avoid this problem, the ratio in Equation 8 may be inverted, resulting into another equation, i.e., $d_{ij}^{ang}[\Delta]* = \left| NN - \sum_{k=1,NN} \left(a\_j[k+\Delta]/a\_i[k]\right)^{-1} \right|$. As this equation is included to avoid false minimums, the "distance" considering the angular relations (D_{ij}^{ang}) is obtained by:

$$D_{ij}^{ang} = \max(\min(d_{ij}^{ang}[\Delta]), \min(d_{ij}^{ang}[\Delta]*)) . \quad (9)$$

Although the angles in the image planes are not maintained as the viewpoint changes, one metric that associates bigger values of compatibility to similar configurations may be defined. Using the "distance" given by Equation 9, the angular compatibility can be obtained by

$$c_{ij}^{ang} = f_c(\alpha_{ang}, D_{ij}^{ang}) = 1/(1 + \alpha_{ang} D_{ij}^{ang}) . \quad (10)$$

Considering the value of the compatibility obtained from distances relations, as shown in the beginning of section 3.2 (c_{ij}^{dist}), as well as the value obtained from Equation 10, the computation of the compatibility in the matching process may be obtained by $c(i, j) = c_{ij}^{ang} c_{ij}^{dist}$. Note that in this equation no information concerning the RO is included.

3.2.2. Metrics based on the volume of MP

As the volume of the MP determined for (i,j) was used in the calculation of the similarities, it may also be considered in the calculation of the compatibility. Knowing the value of Δ that is solution of Equation 9, NN potential pairs around (i,j) are available and the volume of these NN parallelepipeds can be computed. In the case where the correspondences, and also the RO parameters, are correct, the summation of these NN volumes is zero or near zero. Thus, the compatibility for (i,j) must be strengthened when the summation results in low values and the compatibility, considering epipolar constraints, may be computed by

$$c_{ij}^{epi} = 1/\left[1 + \alpha_{epi}' \sum_{i'□n_i, j'□n_j} V_{MP}(\hat{F}, i', j') \right], \quad (11)$$

where α_{epi}' is analogous to α_{epi} in Equation 7. As consequence, the compatibility considering distance relations, angular relations and epipolar constraints, is obtained by $c(i, j) = c_{ij}^{epi} c_{ij}^{ang} c_{ij}^{dist}$.

4. PROPOSED SOLUTION

The proposed algorithm for the simultaneous solution of the correspondence problem and determination of the RO parameters is summarized in the flowchart show in Figure 4.
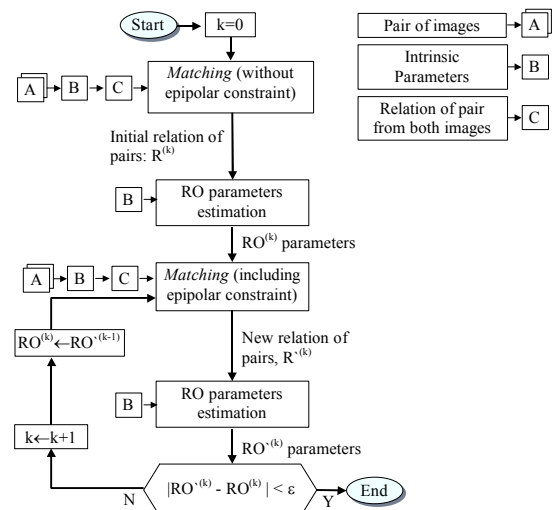

Figure 4: Diagram of the proposed approach.

In that flowchart two matching steps may be observed: one of them executed only once, where the solution of the correspondence problem does not consider the estimates of RO parameters and another one, executed iteratively, in which epipolar constraints are included.

During the first step, where matching is carried out without considering the epipolar constraints, the similarities are computed using the cross-correlation coefficients, the differences of gradient and average intensity as metrics. The compatibility is computed considering the angular and distance relations between neighbors. Based on the result of relaxation labeling, one initial relation of correspondence is established ($R^{(0)}$) and one estimation for the RO is obtained ($RO^{(0)}$).

In the iterative step, the measures of compatibility and similarity are made considering the volume of the MP, besides the metrics used during the first step. At the end of each iteration, a new list of correspondences is obtained, and the RO parameters are recomputed. The process is finished when the RO parameters are considered stable.

4.1. Selection of pairs and dynamic aspects of the solution

Once the relaxation labeling is finished, the selection of pairs should be done. Thus, for each possible value of i (with i$\square$**M**), the value of j$\square$**N** that corresponds to the biggest similarity is chosen as correspondent. To avoid pairs with low similarity, one threshold of similarity is defined (ε_S) and if $p_{ij} < \varepsilon_S$ the pair (i,j) is excluded from the solution.

Ambiguity is another criteria that may be used to exclude some pairs. The ambiguity may be considered by one factor called non-ambiguity factor - NAF [Zha94], which is determined by $NAF_i = 1 - p^{(2nd)}/p^{(1st)}$, where (1st) and (2nd) refer, respectively, to the biggest and the second biggest similarity for point i. According to this concept, if the ratio $p^{(2nd)}/p^{(1st)}$ is small, the NAF will be high, and therefore the ambiguity will be low. Thus, when adopting one threshold for NAF (ε_{NA}), ambiguous pairs may be excluded from the solution.

The threshold for the triangulation error (ε_T) is another criteria that may be used. This threshold is considered to exclude pairs from the solution, where the distance between vectors $\bar{R}_L$ and $\bar{R}_R$ are greater than (ε_T). In that case, the error can be attributed to: the quality of the coordinates, the correspondence and to the RO parameters. As the components of the translation between the cameras are function of the scale adopted and in this work the base component b_x is constraint to 1, ($b_x = 1$), the error in the triangulation is quantified as a percentage of the b_x component.

These thresholds (ε_S, ε_{NA}, ε_T), as well as the dimension of the window for the correlation, the constants α_{grad}, α_{int}, α_{epi}, α'_{epi} and α_{ang}, for example, may be chosen in function of the application and allow the definition of appropriate parameters for different situations and even to classes of images.

Another element that is inherent to relaxation labeling, besides the similarity and compatibility, is the measure of the support of the label j to object i, which is obtained by the product of the compatibility and similarity for a certain neighborhood, as it may be seen in [Hum83, Wu95]. So, the number of elements used in the calculation of the support may also be modified.

One relevant aspect related to the use of constants and thresholds is the possibility of incorporating one dynamic component. The α constant (Equation 4) has an important role in the modification of the metric influence. Assuming by hypothesis that the higher the numbers of correspondent pairs found, the better the quality of the RO parameter is, one may admit that the bigger the ratio between the number of pairs for the matching (considering epipolar constraint) to the initial matching (without epipolar constraint), the bigger is the confidence in the epipolar constraint. So, this idea may be used to incorporate a dynamic component in α_{epi} and α'_{epi}. In this work, it was considered that the values of α_{epi} and α'_{epi} for one iteration i, are respectively function of the initial values of α_{epi} and α'_{epi}, multiplied by the ratio between the number of labeled pairs obtained in the previous iteration by the number of points labeled without considering epipolar constraints.

The tolerance in the triangulation ε_T is another parameter that also may be considered with a dynamic behavior. It is coherent to admit that the triangulation error in the beginning of the process is bigger than in the following iterations. Otherwise, many pairs of points will be eliminated in the beginning of the process. One alternative, used in this work, is to consider a Gaussian function, where the triangulation error for a given iteration is obtained by $\varepsilon_{T_i} = \varepsilon_T e^{-ci}$, where c is a constant that controls the changes in ε_T with the iterations.

Since the solution of the correspondence problem is sensible to images commutation, the proposed approach also considers, for the final solution, only the pairs that belong to independent solutions, i.e., from image pair (I_M,I_N) and (I_N,I_M).

5. IMPLEMENTATION, EXPERIMENTS AND RESULTS

The proposed algorithm for the solution of the correspondence problem, summarized in the

flowchart of Figure 4, was implemented in programs written in language C, for the Unix/Linux operational system.

The experiments carried out aimed to evaluate the behavior of the algorithm for situations where the solution of the correspondence problem is difficult, i.e, in the presence of convergence and rotation; in the presence of repetitive patterns and when the scales are different, as described in section 5.1.

Tests using synthetic and real images were considered to evaluate the algorithm. The synthetic images were generated with POVRAY®, considering different positions of the perspective center and with different angles of convergence for the cameras.

A digital camera Kodak DC40 was used to acquire the real images, being the intrinsic parameters obtained through a calibration procedure, using points located in one invar plate. The software used to compute the intrinsic parameters is based on collinearity equations with additional parameters. The determination of the RO parameters used as reference was obtained by the same calibration program and, in this case, the correspondent pairs of points were provided. Furthermore, in the experiment where influence of repetitive standards is evaluated, a digital video camera was used.

For both, synthetic and real images, the extraction of point entities was made manually, with pixel accuracy. For each image, the extracted entities were stored in the form of a list of points not numbered and not labeled.

In the images of this section, where the pairs of correspondent points are presented as a result of the proposed approach, each labeled pair is marked by one specific pattern, which is not repeated for another pair of points in the image. So, the reader can check visually if the automatic correspondences are correct or not. Based on the number of correctly labeled pairs the algorithm performance can be evaluated.

5.1. Results and Discussion

5.1.1. Influence of convergence and rotation

The evaluation of the influence of the convergence was determined from a set of pairs of images (8 pairs), generated with different angles of convergence and rotation.

The graph of Figure 5 shows that the incorporation of the RO information in the determination of the compatibility and similarity, contributes for the increase in the number of labeled pairs, for all convergence angle considered (up to 30°). Although the variation is not linear, one may observe that the number of labeled pairs is inversely proportional to the convergence. This is an expected behavior, once radiometric and geometric differences, and also the number of occlusions, increase due to the convergence, making the solution of the correspondence more difficult.
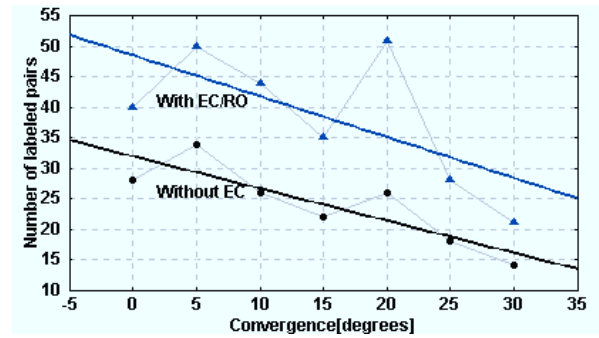

Figure 5: Number of labeled pairs as function of convergence.

Figure 6 shows two sub-images of one pair of images where there is a convergence of 20°, while Figure 7 presents the result of the automatic labeling for the case of another pair where there is a small convergence ($\Delta\varphi=5^o$) but a great rotation ($\Delta\kappa=50^o$).
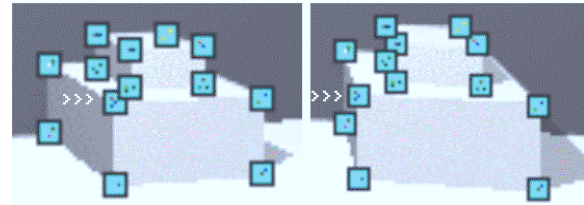

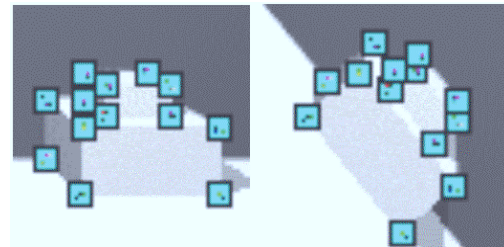Figure 6: Portion of one stereo pair with $\Delta\varphi=20^o$ and the pairs selected automatically by the algorithm.

Figure 7: Labeled pairs for images with $\Delta\varphi=5^o$ and $\Delta\kappa=50^o$.

It may be noticed from these images that despite the effect caused by the change in the viewpoint, the occlusion of some faces are accentuated and all the correspondences are correct.

5.1.2. Influence of repetitive patterns

The evaluation of the algorithm when repetitive patterns are presented was performed using real images acquired by one pair of CCD video cameras.

In Figure 8 it is shown the results obtained for a pair of images that presents repetitive patterns, for two situations.
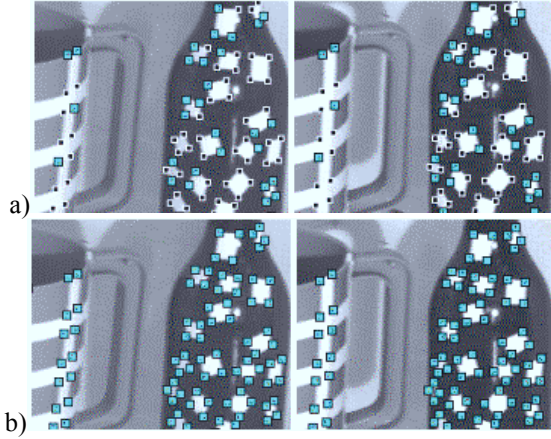
Figure 8: Matching results considering: no epipolar constrains (a) and including epipolar constraint (b).

It is evident from these results that the number of labeled pairs increases significantly with the inclusion of the metrics based on the volume of MP in the compatibility and similarity computation. For these images, the numbers of labeled pairs were 81 and 252, respectively. In the case of the Figure 8b, where all metrics described were considered, 99,2% of the pairs were correctly labeled and only 0,8% were not labeled. The result presented in Figure 8 was obtained considering 6 points in the support calculation. In the case where 3 points were used in the support calculations, the number of labeled pairs falls from 81 to 66 in the matching without epipolar constraints.

In experiments carried out with other images, in the presence of repetitive patterns and also occlusions, the results shows smaller number of labeled pairs and greater number of false correspondence. This result indicates that the algorithm is robust to repetitive patterns but not to occlusions.

5.1.3. Effect of rotation, convergence and scale difference in the algorithm

The evaluation of the influence of convergence, rotation and difference of scale was based on real images. In Figure 9 two pairs of real images are presented, in which five pairs of conjugate epipolar lines, computed by the fundamental matrix obtained by the proposed algorithm, are overlapped to the images.

Results of the labeling process and information concerning the convergence, rotation, scale differences for these two pairs of images can be seen in Table 1.
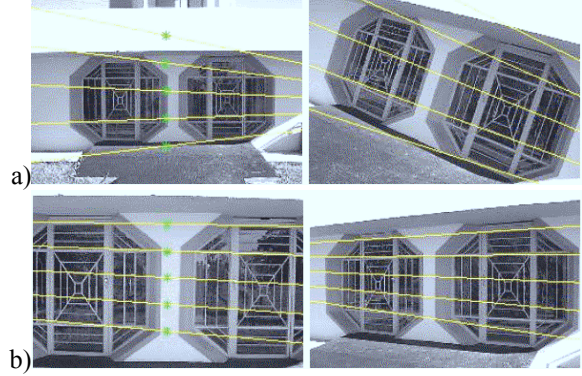

Figure 9: Stereo pairs A/E (a) and C/D (b) affected by scale differences, convergence and rotation.

CHARACTERISTICS		Pair A/E	Pair C/D
Convergence angle		$\cong 26^o$	$\cong 26^o$
Rotation around optical axis		$\cong 20^o$	$\cong 1^o$
Average scale difference		$\cong 33\%$	$\cong 34\%$
Measured points on each image		88/86	71/86
Labeling results:	- corrected	81,4%	57,7%
	- wrong	01,2%	12,7%
	- not labeled	17,4%	29,6%

Table 1: Relaxation labeling results for the stereo pairs show in Figure 9.

It may be observed from the results shown in Table 1 that even when there are scale differences of around 34%, at least 57% of the pairs were correctly labeled. It also may be noticed that although the convergence and scale differences are similar and rotation around optical axis for the pair C/D is small ($\cong 1^o$), the number of occlusion of the pair C/D contributed for the reduction of the number of pairs correctly labeled.

To evaluate the influence of errors of the automatic process of matching on the RO parameters, the pairs of images shown in Figure 9, and other two pairs of the same series were used. The values of the RO parameters obtained for each pair of images were compared to the values obtained during the calibration. The result of this analysis allowed to conclude that for the considered set of images and with 90% of probability, the angular discrepancies in κ, φ and ω are in the interval $[-0,405^o$ to $0,009^o]$ and the discrepancies in the components b_z and b_y are in the interval $[-0,007$ to $0,012]$. The average values of the angular discrepancies and base components are equal to $-0,157^o$ and $-0,003$, respectively. In the discrepancies related to base components, the errors in the b_x component were not considered, once it was constraint to 1 ($b_x=1$).

5.2. Additional considerations

As in the calculation of the reference values for the RO parameters analysis, the lens distortion were modeled, it is reasonable to consider that the obtained discrepancies can be minimized by the inclusion of

the lens distortion parameters in the matrix $I_{\{L,R\}}$ (Section 2).

It is important to observe that some authors consider the matching as an ill-conditioning problem [Hei96]. As consequence, the lack of robustness of the solution for critical situations (convergence, rotation, difference in scales, etc) is a relevant matter. Considering this aspect and that the proposed approach is not in the context of "real-time" applications, the computational complexity of the algorithm, that is function of the number of points extract from both images (m and n), was not discussed.

6. CONCLUSIONS

In this paper it was proposed one method for the solution of point correspondence, together with the estimate of the RO parameter for pairs of images.

It was introduced one metric for compatibility computation based on angular relations and, although these relations are not invariant to viewpoint change, it contributes for the automatic process of matching, once similar structures around candidates are associated to high compatibility.

Added to that, the concept of MP was presented an the volume of this parallelepiped is introduced as metric that allows to include epipolar constraint in the relaxation labeling, eliminating the necessity of explicitly determine the equations of the conjugate epipolar lines and the computation of distances between points candidates to these lines.

The results obtained indicate that when the convergence increases, the algorithm becomes less robust. However, for situations where the images are not acquired in a normal disposal, i.e., with scale differences, convergence, rotations and repetitive patterns; the correspondence and RO parameters estimations may be automated, what contributes for the development of more general 3D reconstruction systems.

Among the relevant points that should be studied in future works one may consider: selection of metrics adequate to classes of images, the inclusion of sub-pixel methods in the point extraction and the incorporation of strategies that takes into account the occlusion of objects.

7. ACKNOWLEDGMENTS

8. REFERENCES

[Bar94] Barakat, H., Doucette, P. and Mikhail, E., Photogrammmetric Analysis of Image Invariance, ISPRS-Commission III-Spatial Information from Digital Photogrammetry and Computer Vision, Munich, September 5-9, pp. 25-34, 1994.

[Fau93] Faugeras, O., Three-Dimensional Computer Vision - a Geometric Viewpoint, The MIT press, Cambridge, 1993.

[Gal97] Galo, M. and Tozzi, C. L., Inclusão de Injunções Epipolares na Solução do Problema de Correspondência, In: Anais do X SIBGRAPI, 1997.

[Gal99] Galo, M. and Tozzi, C. L., The concept of Matching Parallelepiped and it's use in the correspondence problem, ICIP-99/IEEE International Conference on Image Processing, Kobe, pp. 410-414, October, 1999.

[Hab01] Habib, A. and Kelley, D., Automatic relative orientation of large scale imagery over urban areas using modified iterated Hough transform, ISPRS J. of Photogrammetry & Remote Sensing, Vol. 56, pp. 29-41, 2001.

[Häh02] Hähnel, D. and Burgard, W., Probabilistic matching for 3D scan registration, In.: Proc. of the VDI - Conference Robotik 2002 (Robotik), 2002.

[Hei96] Heipke, C., Overview of Image Matching Techniques, OEEPE - Workshop on the application of digital photogrammetric workstations, Lausanne, Switzerland, March 4-7, 1996.

[Hei97] Heipke, C., Automation of Interior, Relative, and Absolute Orientation, ISPRS J. of Photogrammetry & Remote Sensing, Vol. 52, pp. 1-19, 1997.

[Hum83] Hummel, R. A. and Zucker, S. W., On The Foundations of Relaxation Labeling Processes, IEEE-PAMI, Vol. 5, No. 3, pp. 267-287, May, 1983.

[Plu01] Plugers, P., Product survey on Digital Photogrammetric Workstations, GIM International, pp. 69-75, April, 2001.

[Sch89] Schalkoff, R. J., Digital Image Processing and Computer Vision, John Wiley & Sons, Singapore, 1989.

[Sha99] Shao, J., Global image feature correspondence under a multi-image network, Image and Vision Computing, 17, pp. 1021-1030, 1999.

[Tan96] Tang, L. and Heipke, C., Automatic Relative Orientation of Aerial Images, PE&RS, 62 (1), pp. 47-55, January, 1996.

[Zha94] Zhang, Z., Deriche, R., Faugeras, O. and Luong, Q. T., A Robust Technique For Matching Two Uncalibrated Images Through The Recovery of The Unknown Epipolar Geometry, Rapport de Recherche n. 2273, Unité de Recherche INRIA, Shophia-Antipoles, 38p., 1994.

[Wu95] WU, Q. X., A Correlation-Relaxation-Labeling Framework For Computing Optical Flow - Template Matching from a New Perspective, IEEE-PAMI, Vol. 17, No. 8, pp. 843-853, September, 1995.